Spectral dependence of intermolecular distance in organic semiconductors based on FRET theory

FAN KONG*
School of Chemistry and Chemical Engineering, Southeast University, Nanjing 211189, People's Republic of China

The optical properties of N,N'-Diphenyl-N,N'-bis(3-methylphenyl)benzidine (TPD) films doped with tris(8-hydroxyquinoline)aluminum (Alq_3) were studied using absorption and photoluminescence (PL) spectroscopy. A significant spectral overlap between TPD and Alq_3 was observed, which facilitates efficient excitation energy transfer from TPD to Alq_3. Analysis of the PL and PL excitation spectra indicates that the resonant energy transfer is responsible for the high luminescence efficiency of Alq_3 in the hybrid films. Furthermore, the average distance between the donor and acceptor exhibits a linear dependence on the doping concentration, which provides a convenient spectral ruler for exploring intermolecular distances in hybrid semiconductors.

(Received May 16, 2025; accepted December 2, 2025)

Keywords: Organic semiconductors, Photoluminescence, Förster resonance energy transfer, 8-Hydroxyquinoline

1. Introduction

Organic semiconductors have garnered significant interest due to their potential applications in organic light-emitting diodes (OLEDs), lasers, and organic solar cells [1–3]. Among the various strategies for improving the efficiency of optoelectronic devices, dye doping represents an important and facile approach [2,4–6]. In OLEDs, hybrid films containing donors and acceptors are commonly employed as active layers, where resonance energy transfer plays a key role in enhancing device performance. The resonance energy transfer from donor to acceptor typically occurs over nanoscale distances via weak dipole-dipole interactions. Electrons and holes injected from their respective electrodes are transported to the luminescent layer and recombine to form excitons. Excitons generated in the donors can transfer to the acceptors through resonance energy transfer, thereby reducing non-radiative recombination losses. Additionally, doping can improve the balance between electron and hole injection and transport within the hybrid films, leading to higher operational efficiencies in OLEDs [7,8].

Unlike photoexcitation in semiconductor films, the excited states in OLED active layers are formed by electrically injected charge carriers. When N, N'-diphenyl-N, N'-bis(3-methylphenyl) benzidine (TPD) is used as a hole-transport layer, an excess of electrons can combine with holes at the TPD/acceptor interface within a few nanometers, forming excitons that may transfer to acceptors—contributing to high OLED efficiencies [9,10]. In hybrid semiconductor films used in OLEDs, excitons can form in both donors and acceptors. As a result, both Förster resonance energy transfer (FRET) and directly generated excitons in the acceptors contribute to the overall acceptor emission. This typically leads to higher emission intensities from acceptors in electroluminescence spectra compared to photoluminescence (PL) spectra [11,12].

TPD is widely used as a hole-transporting and blue-light-emitting material in OLEDs, and its optical and electrical properties have been extensively studied [13–15]. Doping in TPD films has been shown to significantly enhance luminescence efficiency by suppressing self-quenching. Recent studies on resonance energy transfer in TPD-based conjugated polymers doped with poly(1,4-phenylenevinylene) and the laser dye Fluorol 7GA have demonstrated the potential of such hybrids in novel optoelectronic devices [16,17].

Tris(8-hydroxyquinoline) aluminum (Alq_3) is another key material, serving as both an efficient green emitter and an electron transporter in OLEDs. Active hybrid layers incorporating TPD and Alq_3 have been successfully applied in high-response organic visible-blind ultraviolet detectors [18]. In this study, a series of hybrid TPD films with varying concentrations of Alq_3 were prepared and characterized using absorption and PL spectroscopy. Efficient Förster resonance energy transfer (FRET) from TPD to Alq_3 was observed, leading to a significant increase in the fluorescence quantum efficiency of Alq_3. According to FRET theory, the spectral data indicate a strong linear correlation between the intermolecular distance of the dopants and the doping concentration.

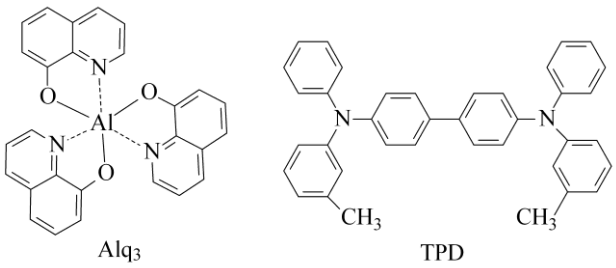

Fig. 1. Chemical structures of Alq_3 and TPD

2. Experimental

The chemical structures of Alq_3 and TPD are presented in Fig. 1. TPD (purchased from Acros Organics) was used as received without further purification. Alq_3 was synthesized in our laboratory and purified via recrystallization in acetone prior to use. TPD and Alq_3 were dissolved separately in tetrahydrofuran (THF) to form the solutions with concentrations of 2 mg/ml and 1 mg/ml, respectively. These solutions were then blended in varying weight ratios of Alq_3 to TPD, specifically 1%, 2%, 5% and 10%.

Thin films of the organic semiconductors were deposited onto clean quartz substrates by spin-coating. To ensure consistent film thickness, the rotation rate and the solution volume dispensed were kept constant for all samples. The PL and PL excitation (PLE) spectra were recorded using a FluoroMax-2 fluorescence spectrophotometer. Absorption spectra were measured with a Shimadzu UV-3100 spectrophotometer. All measurements were carried out at room temperature.

3. Results and discussion

Fig. 2 presents the absorption and PL spectra of the TPD and Alq_3 films. As shown, the absorption spectrum of the TPD film exhibits two peaks at 320 nm and 365 nm, which correspond to $n \rightarrow \pi^*$ and $\pi \rightarrow \pi^*$ electron transitions, respectively. The $n \rightarrow \pi^*$ electron transition originates from the lone pair electrons on nitrogen atoms, while the $\pi \rightarrow \pi^*$ transition arises from the π electrons in the aromatic rings. The PL spectrum of the TPD film shows a peak at 400 nm and a shoulder at around 420 nm, which are attributed to the vibrational replicas of an effective mode of approximately 0.15 eV [19]. The emission spectrum of Alq_3 is centered at 505 nm.

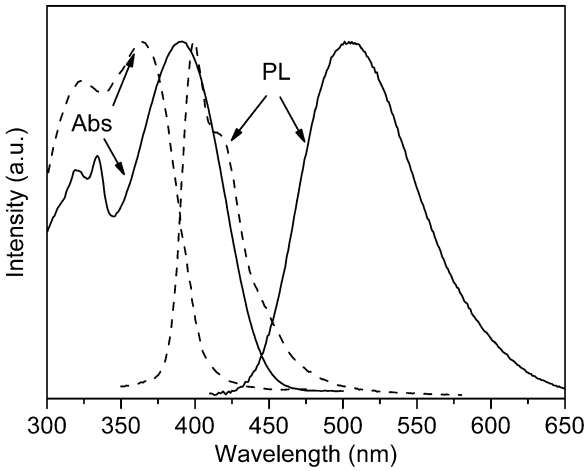

Fig. 2. Absorption and PL spectra of the Alq_3 (solid line) and the TPD (dashed line) films

It can be observed from Fig. 2 that the absorption spectrum of the Alq_3 film, with a maximum at 390 nm, overlaps well with the emission spectrum of the TPD film. This spectral overlap provides favorable conditions for the resonance energy transfer from TPD to Alq_3. According to FRET theory, the Forster radius (R_0) in the TPD/Alq_3 system can be calculated using the following equation (1):

$$R_0^6 = \frac{9000(\ln 10)\kappa^2\Phi_D^0}{128\pi^5 N_A n^4}\int_0^\infty I_D(\lambda)\varepsilon_A(\lambda)\lambda^4 \mathrm{d}\lambda \quad (1)$$

where, κ^2 is the orientation factor, generally taken as 2/3 for random averaging. Φ_D^0 is the fluorescence quantum yield of the pristine TPD film. N_A is Avogadro's constant, n is the average refractive index of the medium in the wavelength range, $I_D(\lambda)$ is the fluorescence intensity of the donor at the wavelength (nm) of λ with the total intensity (area under the curve) normalized to unity, and $\varepsilon(\lambda)$ is the molar absorption coefficient of the acceptor. So, the term $\int_0^\infty I_D(\lambda)\varepsilon_A(\lambda)\lambda^4 \mathrm{d}\lambda$ denotes the spectral overlap integral, which can be evaluated by integrating the overlap between the emission spectrum of TPD and the absorption spectrum of Alq_3. Based on eq. 1 and assuming the values of Φ_D^0 (0.4) and n (1.5) [20,21], the calculated R_0 for the TPD film doped with Alq_3 is 6.08 nm.

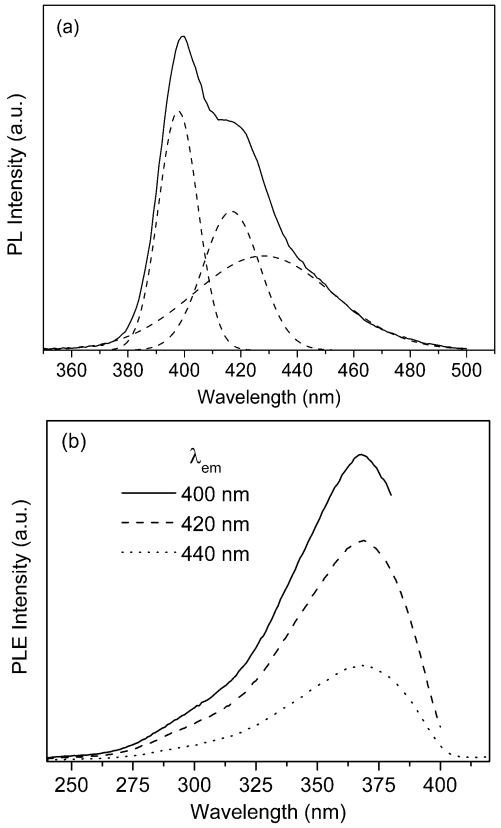

Fig. 3. (a) Gaussian fitting PL spectrum of the TPD film, b) PLE spectra of the TPD film measured at the different monitoring emission wavelengths

The structured PL spectrum of the TPD film can be fitted with three Gaussian bands centered at 398 nm, 416 nm and 428 nm, as shown in Fig. 3a. To investigate the origin of the excited states in TPD, the PLE spectra were measured at different monitoring emission wavelengths, as presented in Fig. 3b. It can be observed that the PLE spectra exhibit identical peak positions at 365 nm, though with varying emission intensities. This indicates that the excited states with different energies arise from the same photoexcitation process. Notably, compared to the absorption spectrum, the peak at 320 nm is absent in the PLE spectra, suggesting that the $n \rightarrow \pi^*$ electron transition does not contribute to the emission from the TPD film. Therefore, the PL of the TPD film originates solely from the $\pi \rightarrow \pi^*$ electron transition.

Fig. 4a presents the PL spectra of the TPD films doped with Alq_3 under photoexcitation at 365 nm using a Xe lamp. As the Alq_3 content in the hybrid films increases, the PL intensity at 400 nm decreases, while the emission at 505 nm is significantly enhanced. Obviously, the emission bands with the PL peaks at 400 nm and 505 nm are attributed to the radiative recombination of excited states in TPD and Alq_3, respectively. Although Alq_3 exhibits some absorption at 365 nm according to Fig. 2, its low concentration in the hybrid system (less than 10 wt%) implies that absorption at this wavelength is dominated by electron transitions in TPD (>95%). Therefore, the enhanced emission from Alq_3 in the hybrid films can be primarily ascribed to resonance energy transfer from TPD to Alq_3. This energy transfer process is further supported by the PLE spectra of the hybrid films.

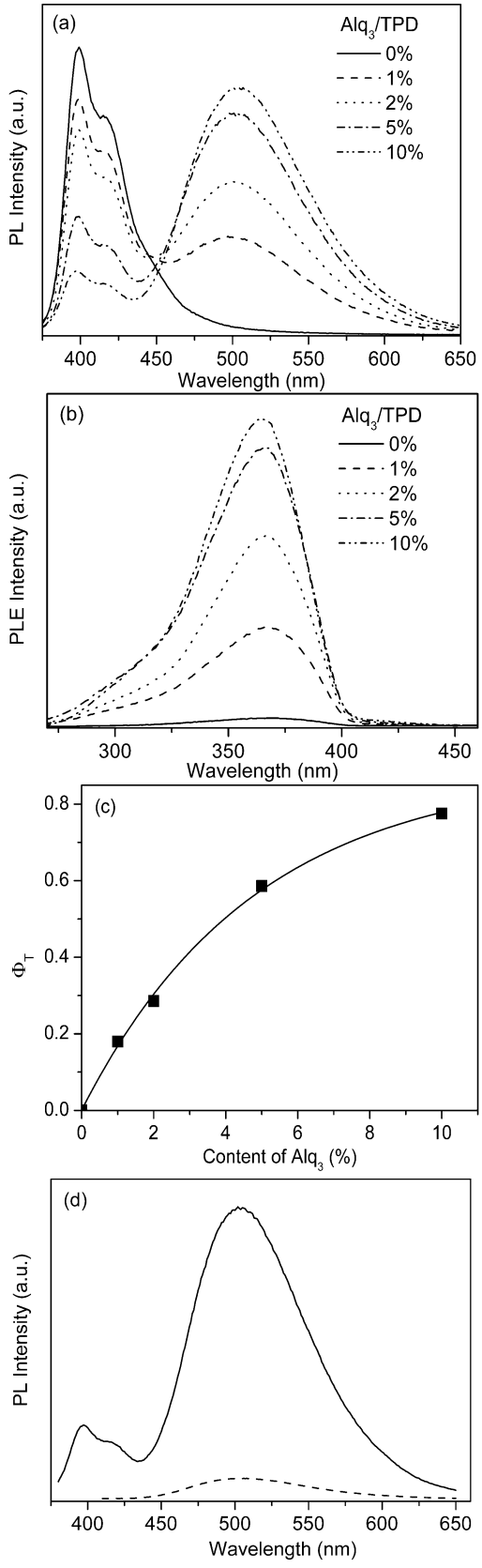

Fig. 4. (a) PL spectra, b) PLE spectra, c) Energy transfer efficiency in the TPD/Alq_3 films, (d) PL spectra of the TPD/Alq_3 (w/w, 10%) film photoexcited at 365 nm (solid line) and 400 nm (dashed line), respectively

Fig. 4b displays the PLE spectra monitored at 505 nm for the TPD films doped with different concentrations of Alq_3. The pristine TPD film shows very weak PLE intensity at this wavelength. Given the PL spectra of TPD and Alq_3 in Fig. 2, the emission at 505 nm can be reasonably assigned to the radiative recombination of Alq_3 excited states in the hybrid films. All the PLE spectra exhibit a consistent peak at 365 nm, corresponding to the absorption maximum of TPD. The PLE intensity at 365 nm increases considerably with higher Alq_3 content, indicating that photoexcitation of TPD contributes effectively to the emission from Alq_3 in the hybrid films. Under 365 nm excitation, the excited states are generated in TPD via the $\pi \rightarrow \pi^*$ electron transitions, followed by resonance energy transfer to Alq_3 prior to spontaneous radiative or nonradiative recombination in TPD. As a result, the emission intensity of Alq_3 is markedly enhanced in the hybrid films.

The energy transfer efficiency (Φ_T) can be determined by quantifying the quenching of the donor emission in the presence of the acceptor. The reduced emission from TPD is indicative of resonance energy transfer to Alq_3, Thus, Φ_T can be calculated based on the PL intensity of TPD in the absence and presence of Alq_3, as described by the following equation (2):

$$\Phi_T = 1 - \frac{\int_0^\infty I_D(\lambda) d\lambda}{\int_0^\infty I_D^0(\lambda) d\lambda} \tag{2}$$

$I_D^0(\lambda)$ and $I_D(\lambda)$ are the PL intensities of TPD at the emission wavelength of λ in the absence and presence of Alq_3, respectively. Fig. 4c shows the energy transfer efficiencies calculated for the TPD/Alq_3 hybrid films calculated using eq. 2. The Φ_T value reaches 77.6% in the hybrid film with a dopant concentration of 10%. The efficient transfer of excitations from TPD to Alq_3 contributes significantly to enhancing the fluorescence quantum efficiency of Alq_3 in the hybrid films.

Fig. 4d displays the PL spectra of the TPD/Alq_3 (w/w, 10%) hybrid film under photoexcitation at 365 nm and 400 nm, respectively. The PL intensity at 505 nm obtained by excitation at 365 nm is approximately 18 times higher than that at 400 nm. According to the absorption spectra of the TPD and Alq_3 films shown in Fig. 2, the excitation at 400 nm lies near the absorption edge of TPD, but coincides closely with the maximum absorption of Alq_3. Therefore, when excited at 400 nm, the emission from the hybrid film primarily results from direct photoexcitation of Alq_3. As discussion above, the excitation at 365 nm is predominantly absorbed by TPD in the hybrid film. In this case, the excited states generated in TPD are efficiently transferred to Alq_3 though dipole-dipole interactions, leading to the enhanced emission from Alq_3 via resonance energy transfer. Consequently, the fluorescence quantum efficiency of Alq_3 is significantly improved. This explains the strongly enhanced Alq_3 emission observed in the PL spectrum of the hybrid film when excited at the absorption maximum of TPD.

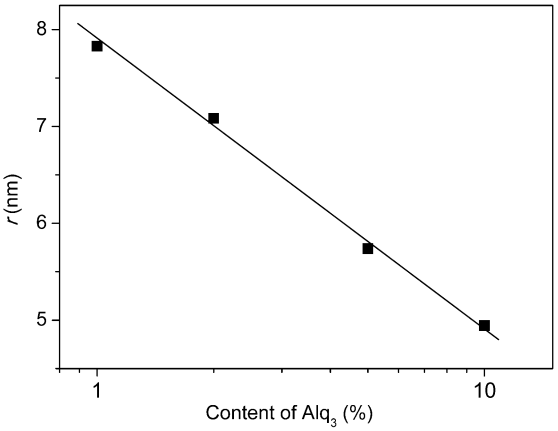

Fig. 5. Average distance (r) between the donor and acceptor

The FRET theory serves as a spectral ruler for measuring intermolecular distances, enabling precise quantification at the nanoscale (typically 1–10 nm) through analysis of the energy transfer efficiency between donor and acceptor. The average distance (r) between the donor and acceptor in the hybrid membrane can be calculated according to the following equation:

$$\Phi_T = \frac{1}{1 + (r / R_0)^6} \tag{3}$$

As shown in Fig. 5, the average donor–acceptor distance in the hybrid film exhibits a strong linear correlation with the doping concentration. This ability to transform nanoscale molecular dynamics into quantifiable spectral signals is of significant importance. FRET technology thus offers a powerful tool for life sciences and materials science, facilitating not only the clarification of static molecular structures but also the decoding of their dynamic behaviors [22,23].

4. Conclusions

This study elucidates the FRET process between TPD and Alq_3 through investigating the optical properties of Alq_3-doped TPD films. The efficient resonance energy transfer significantly enhances the luminescence efficiency of Alq_3. By quantitatively analyzing the PL quenching of TPD, the FRET efficiency has been accurately determined, enabling the calculation of the average donor-acceptor distance based on Förster theory. A strong linear correlation has been observed between the average intermolecular distance and the doping concentration in the hybrid films. The findings establish a straightforward methodology for developing spectral rulers based on FRET, providing valuable insights for the design and optimization of organic optoelectronic

materials.

Conflict of Interest

The author declares no conflict of interest.

References

[1] G. Li, M. C. Tseng, Y. Chen, S. Y. Yeung, H. He, Y. Cheng, J. Cai, E. Chen, H. S. Kwok, Light Sci. Appl. **13**(12), 301 (2024).
[2] Y. Jiang, Y. Y. Liu, X. Liu, H. Lin, K. Gao, W. Y. Lai, W. Huang, Chem. Soc. Rev. **49**(16), 5885 (2020).
[3] J. C. Yi, G. Y. Zhang, H. Yu, H. Yan, Nat. Rev. Mater. **9**(1), 46 (2024).
[4] T. H. Liu, C. Y. Iou, C. H. Chen, Curr. Appl. Phys. **5**(3), 218 (2005).
[5] W. M. Su, W. L. Li, Z. R. Hong, M. T. Li, T. Z. Yu, B. Chu, B. Li, Z. Q. Zhang, Z. Z. Hu, Appl. Phys. Lett. **87**(21), 213501 (2005).
[6] Y. W. Park, Y. M. Kim, J. H. Choi, T. H. Park, J. W. Huh, H. S. Kim, M. J. Cho, D. H. Choi, B. K. Ju, Appl. Phys. Lett. **95**(14), 143305 (2009).
[7] U. Deori, G. P. Nanda, C. Murawski, P. Rajamalli, Chem. Sci. **15**(43), 17739 (2024).
[8] T. H. Ha, J. Y. Yoo, C. W. Lee, Chem. Eng. J. **503**, 158323 (2025).
[9] J. Chan, A. D. Rakic, C. Y. Kwong, Z. T. Liu, A. B. Djurisic, M. L. Majewski, W. K. Chan, P. C. Chui, Smart Mater. Struct. **15**(1), S92 (2006).
[10] H. Mu, W. Li, R. Jones, A. Steckl, D. Klotzkin, J. Lumin. **126**(1), 225 (2007).
[11] J. Liu, Q. G. Zhou, Y. X. Cheng, Y. H. Geng, L. X. Wang, D. G. Ma, X. B. Jing, F. S. Wang, Adv. Funct. Mater. **16**(7), 957 (2006).
[12] C. F. Huebner, R. D. Roeder, S. H. Foulger, Adv. Funct. Mater. **19**(22), 3604 (2009).
[13] T. Tsuboi, A. K. Bansal, A. Penzkofer, Thin Solid Films **518**(2), 835 (2009).
[14] T. Yamada, T. Sato, K. Tanaka, H. Kaji, Org. Electron. **11**(2), 255 (2010).
[15] S. R. Mohan, M. P. Joshi, M. P. Singh, Chem. Phys. Lett. **470**(4-6), 279 (2009).
[16] B. A. Al-Asbahi, Phys. Scr. **98**(9) 095908 (2023).
[17] B. A. Al-Asbahi, Opt. Quant. Electron. **56**(6), 930 (2024).
[18] D. Ray, K. L. Narasimhan, Appl. Phys. Lett. **91**(9), 093516 (2007).
[19] I. Vragovic, E. M. Calzado, M. A. Garcia, Chem. Phys. **332**(1), 48 (2007).
[20] T. Tsuboi, A. K. Bansal, A. Penzkofer, Thin Solid Films **518**(2), 835 (2009).
[21] A. Basir, H. Alzahrani, K. Sulaiman, F. F. Muhammadsharif, A. Y. Mahmoud, R. R. Bahabry, M. S. Alsoufi, T. M. Bawazeer, S. F. Ab Sani, Physica B **606**, 412816 (2021).
[22] S. Hirashima, S. Park, H. Sugiyama, Chem. Eur. J. **29**(24), e20220396 (2023).
[23] J. Q. Thou, J. Y. Li, C. Cheng, Y. J. Yao, Y. Li, H. Liu, L. Y. Wu, Int. J. Biol. Macromol. **274**(1), 133266 (2024).

*Corresponding author: kongfan@seu.edu.cn